

EFFECT OF ASPECT RATIO OF ENCLOSURE ON FREE CONVECTION FROM HORIZONTAL CYLINDERS IN BINGHAM PLASTIC FLUIDS

Ashok Kumar Baranwal^{1*}, Anoop Kumar Gupta², Anurag Kumar Tiwari³,
Roderick Melnik^{4,5}

¹Department of Chemical Engineering, BIT Sindri, Dhanbad 828123, India

²Department of Chemical and Biochemical Engineering, IIT Patna 801106, India

³Department of Chemical Engineering, NIT Jalandhar 144011, India

⁴Wilfrid Laurier University, 75 University Avenue West, Waterloo, Ontario, Canada

⁵BCAM Basque Center for Applied Mathematics, Bizkaia, Spain

Heat transfer in steady free convection from differentially heated cylinders enclosed in a rectangular duct filled with Bingham plastic fluids has been solved numerically for the ranges of the dimensionless groups as, Rayleigh number, $10^2 \leq Ra \leq 10^6$; Prandtl number, $10 \leq Pr \leq 100$ and, Bingham number, $0 \leq Bn \leq 50$ for aspect ratios $AR = 0.5, 0.6, 0.7, 0.8, 0.9$ and 2 . The streamlines, isotherm contours, yield surfaces, local and average Nusselt numbers were analysed and discussed. It is found that as the aspect ratio of the enclosure increases from 0.5 to 0.9 , the average Nusselt number on the surface of the hot cylinder increases as a larger amount of fluid takes part in convection. Moreover, at sufficiently large Bingham numbers, yield stress forces dominate over buoyancy causing the flow to cease and thus the Nusselt number approaches its conduction limit. Finally, the Nusselt number approaches its conduction limit once the maximum Bingham number is reached.

Keywords: Bingham plastic fluids, aspect ratio, Rayleigh number, Nusselt number, natural convection

1. INTRODUCTION

Suspensions, emulsions, foams, gels, etc., such fluids exhibit yield stress (Barnes and Walters, 1985; Bird et al., 1983). The dual nature of these fluids not only poses challenges in homogenization and mixing (Chhabra and Richardson, 2008; Paul et al., 2004) but also impedes heat transfer in such systems (Chhabra and Richardson, 2008). Heat transfer mechanism is conduction and convection in the unyielded (solid-like) and yielded (fluid-like) domains, respectively.

Considerable literature is now available for the enclosure walls at different types of boundary conditions (Turan et al., 2012), geometrical arrangement, e.g., cylinders placed along an x -axis (Park et al., 2012), or on the diagonal duct (Lee et al., 2010), or vertically aligned (Yoon et al., 2014) and enclosure aspect

* Corresponding author, e-mail: akb.che@bitsindri.ac.in

<https://journals.pan.pl/cpe>

Presented at the International Chemical Engineering Conference 2021 (ICHEEC): 100 Glorious Years of Chemical Engineering and Technology, held from September 16–19, 2021 at Dr B. R. Ambedkar National Institute of Technology, Jalandhar, Punjab, India.



© 2022. The Author(s). This is an open-access article distributed under the terms of the Creative Commons Attribution (CC-BY 4.0, <https://creativecommons.org/licenses/by/4.0/>), which permits unrestricted use, distribution, and reproduction in any medium, provided the original author and source are credited.

ratio (Turan et al., 2011). Recently, the results of the natural convection have been summarised for square enclosures with and without internal bodies in Newtonian fluids. The reported results are for the internal objects that are square, circular, and elliptical cylinders (Pandey et al., 2019). Very few results are available for enclosed horizontal circular cylinders inside a square duct in a Bingham fluid (Sairamu et al., 2013). Also, some results are available for differentially heated system along the vertical and diagonal of the square enclosure maintained at isothermal conditions in Bingham plastic fluids (Mishra and Chhabra, 2020). The rectangular enclosure has been solved for the range of $10^4 \leq Ra \leq 10^6$, $1/8 \leq AR \leq 8$ at $Pr = 7$ (Turan et al., 2011). So far, natural convection from two internal cylinders enclosed in the rectangular duct of different aspect ratios is not solved. Albeit, this has many practical applications such as in solar collectors, in heating and preservation of canned foods, in electronic equipment cooling and in energy storage and conservation. The objective is to fill this research gap.

2. PROBLEM STATEMENT AND EQUATIONS

Figure 1 is conducted for different aspect ratio values ($AR = H/L$) of the rectangular enclosure at a constant value of R , i.e., $R/L = 0.2$. Height of the enclosure is varied to achieve a range of aspect ratios keeping width as fixed. One cylinder surface is hot (at temperature T_h) while the other cylinder surface is cold (at temperature T_c). Since the maximum temperature difference (between fluid at initial and hot surface) applied is 5K; therefore, the fluid thermophysical properties are not dependent on temperature. The Boussinesq approximation $\rho_c - \rho = \rho_c \beta (T - T_c)$ is used to model the density. In dimensionless formulations, the mass, momentum and heat transfer equations are (Baranwal and Chhabra, 2017):

Continuity equation:

$$\frac{\partial U_x}{\partial x} + \frac{\partial U_y}{\partial y} = 0 \quad (1)$$

x-momentum equation:

$$\left(\frac{\partial (U_x U_x)}{\partial x} + \frac{\partial (U_x U_y)}{\partial y} \right) = -\frac{\partial p}{\partial x} + \sqrt{\frac{Pr}{Ra}} \left(\frac{\partial \tau_{xx}}{\partial x} + \frac{\partial \tau_{yx}}{\partial y} \right) \quad (2)$$

y-momentum equation:

$$\left(\frac{\partial (U_y U_x)}{\partial x} + \frac{\partial (U_y U_y)}{\partial y} \right) = -\frac{\partial p}{\partial y} + \theta + \sqrt{\frac{Pr}{Ra}} \left(\frac{\partial \tau_{xy}}{\partial x} + \frac{\partial \tau_{yy}}{\partial y} \right) \quad (3)$$

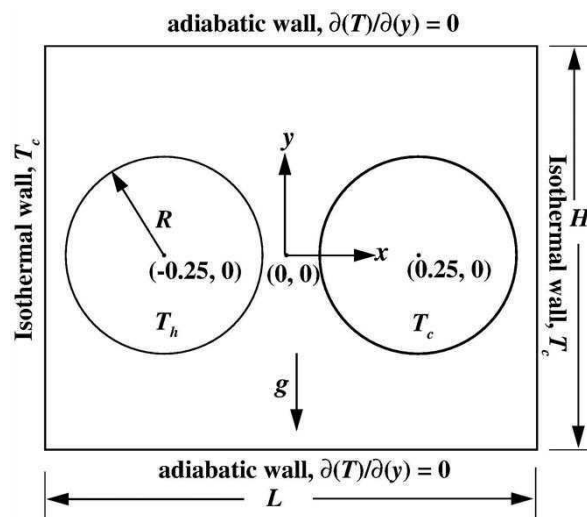


Fig. 1. Geometric representation of the physical domain

Energy equation:

$$\frac{\partial (U_x \theta)}{\partial x} + \frac{\partial (U_y \theta)}{\partial y} = \frac{1}{\sqrt{\text{Pr Ra}}} \left(\frac{\partial^2 \theta}{\partial x^2} + \frac{\partial^2 \theta}{\partial y^2} \right) \quad (4)$$

The extra stress tensor in non-dimensional form is expressed as (Bird et al., 1987):

$$\tau = \left(1 + \frac{\text{Bn}}{|\dot{\gamma}|} \right) \dot{\gamma}, \quad \text{if } |\tau| > \text{Bn} \quad (5a)$$

$$\dot{\gamma} = 0, \quad \text{if } |\tau| \leq \text{Bn} \quad (5b)$$

Because Eqs. (5a) and (5b) together are non-differentiable and discontinuous, it is important to use an appropriate continuous form of this equation (Glowinski and Wachs, 2011). Two regularization approaches are widely used (O'Donovan and Tanner, 1984; Papanastasiou, 1987) to overcome this difficulty. These approaches can be written as follows:

Papanastasiou model:

$$\tau = \left(1 + \frac{[1 - \exp(-M |\dot{\gamma}|)] \text{Bn}}{|\dot{\gamma}|} \right) \dot{\gamma} \quad (6)$$

where M is the regularization parameter.

Bi-viscous model:

$$\tau = \frac{\mu_y}{\mu_B} \dot{\gamma}, \quad \text{if } |\tau| < \text{Bn} \quad (7a)$$

$$\tau = 1 + \left[1 - \left(\frac{1}{\frac{\mu_y}{\mu_B}} \right) \right] \frac{\text{Bn}}{|\dot{\gamma}|}, \quad \text{if } |\tau| \geq \text{Bn} \quad (7b)$$

where μ_y is the yielding viscosity.

The no-slip boundary condition is used on all solid boundaries. For temperature, $\theta = 0$ is on the cold surface and the vertical walls, $\partial\theta/\partial y = 0$ is on the horizontal walls, and $\theta = 1$ is on the hot surface. U_r ($= \sqrt{Lg\beta\Delta T}$) and L are used for the reference scales. Thus, the stress, shear rate, and pressure are all scaled as $\mu_B (U_r/L)$, U_r/L and $\rho_c U_r^2$, respectively.

3. NUMERICAL METHODOLOGY

Here, COMSOL Multiphysics software is used to solve the problem numerically. The flow domain is meshed with the free triangular elements of different refinements (G1, G2 and G3). 10^{-5} is used as the relative convergence criterion to terminate the simulations. The results of drag and Nu_{avg} with the grids G2 and G3 are obtained identical, and therefore, G2 grid elements 39200 and 95040 have been used for $AR = 0.5$ and 2 respectively.

4. RESULTS AND DISCUSSION

4.1. Validation of results

Figure 2 shows a comparison for Nu_{avg} along the hot wall and a temperature distribution along the midline of the enclosure, parallel to the x -axis in a Bingham plastic fluid (Turan et al., 2011). The present and literature values are seen to superimpose each other showing the new results to be independent of numerical artefacts.

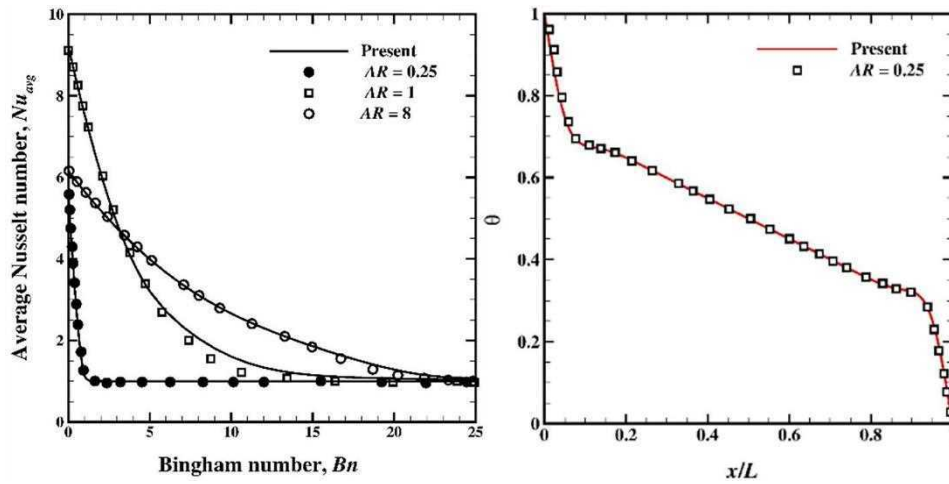


Fig. 2. Comparison of the present results; (lines) with literature (Turan et al., 2011) and (symbols) at $Ra = 10^6$, $Pr = 7$ in Bingham plastic fluids

4.2. Streamlines and isotherm contours

For the extreme case of $AR = 0.5$, Fig. 3(i)(a), the four recirculating regions are formed even at very low Bn . Everywhere flow domain is unyielded for $Bn \geq 0.05$ at $Ra = 10^2$. Bn_{max} value for $Ra = 10^6$ is

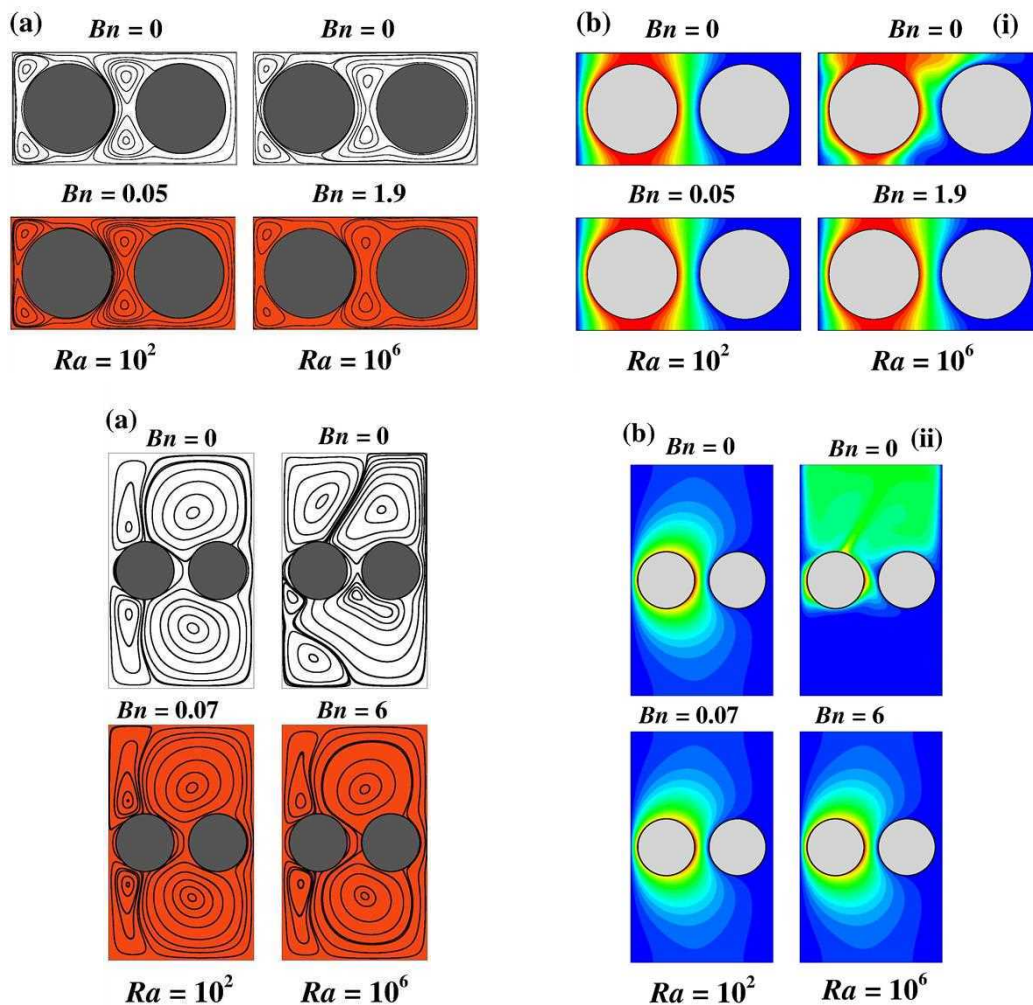


Fig. 3. Representative streamlines (a) and isotherm contours; (b) at $Pr = 10$ (shaded part-unyielded portions) for (i) $AR = 0.5$ and (ii) $AR = 2$

~ 1.9 . The recirculating zones are same for $AR = 0.9$ as well except that a larger proportion of the fluid participates in heat transfer. For the $AR = 2$, one can observe similar trends only the different thing is that as increase the AR , the recirculation zone becomes bigger. The value of Bn_{\max} increases as AR increases for all Rayleigh number. Effect of AR is more pronounced on Bn_{\max} at $Ra = 10^6$ than that of at $Ra = 10^2$. In the isotherms above and below, the cold cylinder mass is almost at $\theta = 0$ that indicating negligible heat transfer. Heat transfer is facilitated when the aspect ratio increases for $AR \leq 1$ because more amount of fluid participates in the convection.

4.3. Average Nusselt number

For all cases of AR , at $Ra = 100$, the results are not affected by Bn because of poor convection as shown in Fig. 4. At another aspect ratio, as the size of the enclosure increases, which promotes heat transfer at least up to $AR = 0.9$. Even at smaller AR ($= 0.5$), a sufficient amount of fluid is present which modifies the heat transfer pattern. Bn differs in each case indicating that the fluid yield stress has a significant impact on rate of heat transfer. Moreover, effect of the Bn is more pronounced at larger aspect ratio values. Heat transfer rate decreases with rising Bn at fixed values of Ra , Pr , and AR , and it approaches the limit for pure conduction when $Bn = Bn_{\max}$.

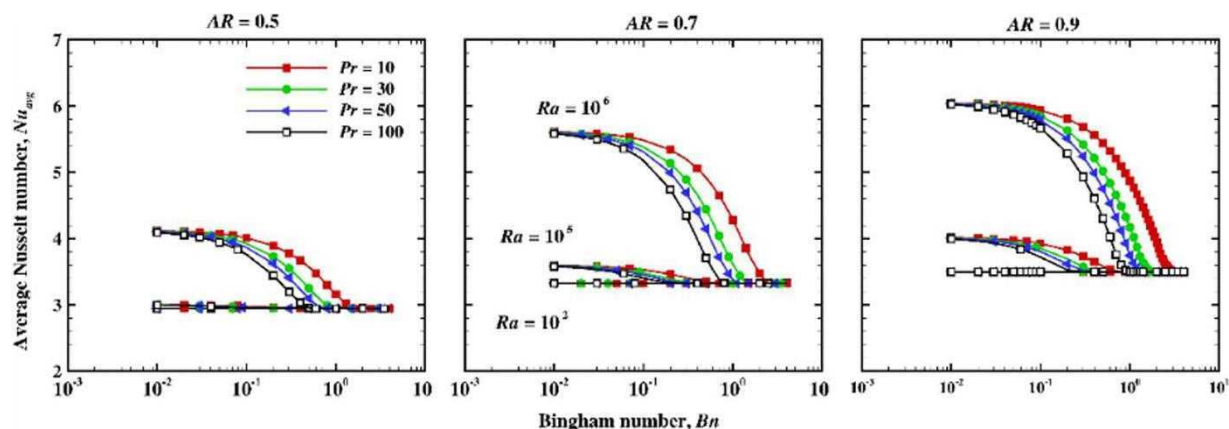


Fig. 4. Dependence of the Nu_{avg} on Bn , Pr , and Ra for the heated cylinder

This pattern is obtained for all AR , except that Ra and Pr modulate rate of approach towards pure conduction. In addition, with rising Bn , Nu_{avg} drops from its value at $Bn = 0$ to pure conduction depending on the value of AR .

5. CONCLUSIONS

The numerical analysis of two-cylinder system inside a rectangular duct with various aspect ratios has been carried out. The streamlines, isotherm contours, yield surfaces, local and average Nusselt numbers are included in the results. The free convection heat transfer results have been presented to elucidate the effect of the dimensionless numbers. The variation in the aspect ratio of the enclosure is sufficient to modify the heat transfer pattern. The mode of heat transfer in solid zones is primarily by conduction while convection occurs in fluid-like zones. Nu_{avg} follows an opposite dependence on the Bn and Pr , whereas it confirms positive support on Ra . Also, the geometrical configuration of the enclosure increasingly promotes heat transfer at least up to $AR = 0.9$. It is seen that the effect of the Bn is more considerable at larger aspect ratio values.

SYMBOLS

AR	aspect ratio,
c_p	specific heat capacity of fluid, J/(kg·K)
d	diameter of cylinder, m
h	convective heat transfer coefficient, W/(m ² ·K)
M	growth rate parameter, –
Nu_L	local Nusselt number, $\frac{h \cdot L}{k}$
Nu_{avg}	average Nusselt number, $\frac{1}{S} \int_S Nu dS$
p	pressure, –
U_x, U_y	x - and y -components of the velocity, –
S	surface area, m ²

Greek symbols

β	coefficient of volume expansion, 1/K
$\dot{\gamma}$	rate of strain tensor, –
μ_B	Bingham plastic viscosity, Pa·s
ρ	density of the fluid, kg/m ³
ρ_c	fluid density, T_c , kg/m ³
θ	temperature, $\theta = (T - T_c)/(T_h - T_c)$, –
τ	yield stress, Pa

REFERENCES

- Baranwal A.K., Chhabra R.P., 2017. Effect of fluid yield stress on natural convection from horizontal cylinders in a square enclosure. *Heat Transfer Eng.*, 38, 557–577. DOI: [10.1080/01457632.2016.1200373](https://doi.org/10.1080/01457632.2016.1200373).
- Barnes H.A., Walters K., 1985. The Yield Stress Myth? *Rheol. Acta*, 24, 323–326. DOI: [10.1007/BF01333960](https://doi.org/10.1007/BF01333960).
- Bird R.B., Armstrong R.C., Hassager O., 1987. *Dynamics of polymeric liquids. Volume 1: Fluid dynamics*. 2nd edition, Wiley, New York.
- Bird R.B., Dai G.C., Yarusso B.J., 1983. The rheology and flow of viscoplastic materials. *Rev. Chem. Eng.*, 1, 1–70. DOI: [10.1515/revce-1983-0102](https://doi.org/10.1515/revce-1983-0102).
- Chhabra R. P., Richardson J. F., 2008. *Non-Newtonian flow and applied rheology*. 2nd edition, Butterworth-Heinemann, Oxford, UK. DOI: [10.1016/B978-0-7506-8532-0.X0001-7](https://doi.org/10.1016/B978-0-7506-8532-0.X0001-7).
- Glowinski R., Wachs A., 2011. On the numerical simulation of viscoplastic fluid flow. *Handbook of Numerical Analysis*, 16, 483–717. DOI: [10.1016/B978-0-444-53047-9.00006-X](https://doi.org/10.1016/B978-0-444-53047-9.00006-X).
- Lee J.M., Ha M.Y., Yoon H.S., 2010. Natural convection in a square enclosure with a circular cylinder at different horizontal and diagonal locations. *Int. J. Heat Mass Transfer*, 53, 5905–5919. DOI: [10.1016/j.ijheatmasstransfer.2010.07.043](https://doi.org/10.1016/j.ijheatmasstransfer.2010.07.043).
- Mishra L., Chhabra R.P., 2020. Combined effects of fluid yield stress and geometrical arrangement on natural convection in a square duct from two differentially heated horizontal cylinders. *J. Therm. Sci. Eng. Appl.*, 12, 011016. DOI: [10.1115/1.4044429](https://doi.org/10.1115/1.4044429).
- O'Donovan E.J., Tanner R.I., 1984. Numerical study of the Bingham squeeze film problem. *J. Non-Newtonian Fluid Mech.*, 15, 75–83. DOI: [10.1016/0377-0257\(84\)80029-4](https://doi.org/10.1016/0377-0257(84)80029-4).
- Pandey S., Park Y.G., Ha M.Y., 2019. An exhaustive review of studies on natural convection in enclosures with and without internal bodies of various shapes. *Int. J. Heat Mass Transfer*, 138, 762–795. DOI: [10.1016/j.ijheatmasstransfer.2019.04.097](https://doi.org/10.1016/j.ijheatmasstransfer.2019.04.097).

- Papanastasiou T.C., 1987. Flow of materials with yield. *J. Rheol.*, 31, 385–404. DOI: [10.1122/1.549926](https://doi.org/10.1122/1.549926).
- Park Y.G., Yoon H.S., Ha M.Y., 2012. Natural convection in square enclosure with hot and cold cylinders at different vertical locations. *Int. J. Heat Mass Transfer*, 55, 7911–7925. DOI: [10.1016/j.ijheatmasstransfer.2012.08.012](https://doi.org/10.1016/j.ijheatmasstransfer.2012.08.012).
- Paul E.I., Atiemo-Obeng V.A., Kresta S.M., 2004. *Handbook of industrial mixing: Science and practice*. Wiley, Hoboken, NJ.
- Sairamu M., Nirmalkar N., Chhabra R.P., 2013. Natural convection from a circular cylinder in confined Bingham plastic fluids. *Int. J. Heat Mass Transfer*, 60, 567–581. DOI: [10.1016/j.ijheatmasstransfer.2013.01.024](https://doi.org/10.1016/j.ijheatmasstransfer.2013.01.024).
- Turan O., Poole R.J., Chakraborty N., 2011. Aspect ratio effects in laminar natural convection of Bingham fluids in rectangular enclosures with differentially heated side walls. *J. Non-Newtonian Fluid Mech.*, 166, 208–230. DOI: [10.1016/j.jnnfm.2010.12.002](https://doi.org/10.1016/j.jnnfm.2010.12.002).
- Turan O., Poole R.J., Chakraborty N., 2012. Boundary condition effects on natural convection of Bingham fluids in a square enclosure with differentially heated horizontal walls. *Comput. Therm. Sci.: Int. J.*, 4, 77–97. DOI: [10.1615/ComputThermalScien.2012004759](https://doi.org/10.1615/ComputThermalScien.2012004759).
- Yoon H.S., Park Y.G., Jung J.H., 2014. Natural convection in a square enclosure with differentially heated two horizontal cylinders. *Numer. Heat Transfer, Part A*, 65, 302–326. DOI: [10.1080/10407782.2013.831679](https://doi.org/10.1080/10407782.2013.831679).

Received 16 February 2022

Received in revised form 9 April 2022

Accepted 11 April 2022